FISEVIER

Contents lists available at ScienceDirect

#### Bioresource Technology

journal homepage: www.elsevier.com/locate/biortech





# Addition of *in situ* clay catalysts at different process points in a cascaded hydrothermal carbonization-pyrolysis process for agro-industrial waste valorization

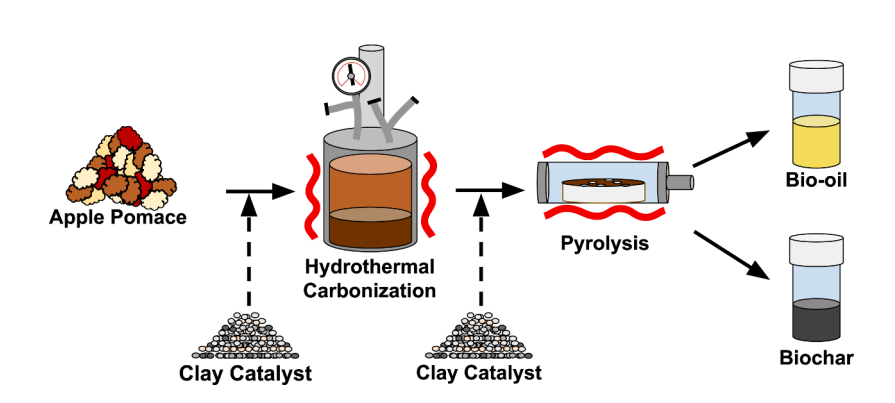
James L. Adair<sup>1</sup>, Madeline Karod<sup>1</sup>, Jillian L. Goldfarb<sup>\*</sup>

Cornell University, Department of Biological & Environmental Engineering, 111 Wing Drive, Ithaca, NY 14853, USA

#### HIGHLIGHTS

- Cascaded hydrothermal carbonization (HTC) followed by pyrolysis of apple pomace.
- Added clay catalyst either prior to HTC or to hydrochar prior to pyrolysis.
- Bio-oils made from hydrochar + clay have higher aldehyde concentration.
- Bio-oils from clay-catalyzed hydrochars have more ketones and hydrocarbons.
- Clay added prior to HTC decreases surface area of pyrolyzed biochars.

#### G R A P H I C A L A B S T R A C T



#### ARTICLE INFO

Keywords: Hydrothermal carbonization Pyrolysis Clay catalyst Biochar Bio-oil

#### ABSTRACT

Agro-industrial wastes can be thermochemically converted to sustainable fuels and upcycled carbon products. However, processing such feedstocks through pyrolysis or hydrothermal carbonization (HTC) alone yields fuels that require significant downstream upgrading. In this work, apple pomace was treated via a cascaded HTC-pyrolysis process using inexpensive and abundant clay catalysts, montmorillonite and attapulgite. Clays were added pre-HTC to raw biomass or to hydrochar pre-pyrolysis to examine the effect of addition as a function of process insertion point. Both clays produce similar bio-oils when they are added at the same process point. However, bio-oil was affected by the point in which clay was added to the process (before or after HTC). When clay was added pre-HTC, the bio-oil had an average hydrocarbon content twice that when clay was added to the hydrochar after HTC, prior to pyrolysis.

#### 1. Introduction

As climate change accelerates - atmospheric carbon levels surpassed

420 ppm in May 2022 (IEA, 2022) - global pressure mounts to shift from conventional fossil fuels to renewable energy sources. Hydrothermal Carbonization (HTC), or wet pyrolysis, converts carbonaceous

E-mail address: goldfarb@cornell.edu (J.L. Goldfarb).

<sup>\*</sup> Corresponding author.

<sup>&</sup>lt;sup>1</sup> Equal contribution.

feedstocks to solid hydrochar (HC), liquid biocrude and non-condensable gas (>99 % CO<sub>2</sub>) in aqueous media between 180 and 250 °C, over minutes to hours in a pressurized vessel (Li et al., 2013). This makes HTC well suited to process wet biomass wastes as it leverages the water content of the feedstock. HTC mimics the Earth's coalification processes at an accelerated mass and time scale by concentrating elemental carbon in the biomass feedstock into the solid HC and rejecting oxygen into the liquid and gas phases through a series of hydrolysis, deoxygenation, and decarboxylation reactions. Hydrothermally processed biocrude contains more N and O heteroatoms than its petroleum counterparts, which necessitates significant catalytic upgrading to enhance the biocrude heating value (Posmanik et al., 2017). This can be accomplished *in situ* during HTC with heterogeneous catalysts like pre-fabricated metal-alumina oxide complexes (Ding et al., 2022) and naturally occurring clay minerals (Karod et al., 2022b).

HC is an energetically dense solid fuel, touted as a replacement for coal in energy generation scenarios (Saqib et al., 2018). Despite the coallike heating values and composition of HCs, a reactive amorphous secondary char (SC) often forms on the surface of the solid HC during carbonization (Volpe et al., 2018). This SC may limit the use of these "bio-coals" as drop-in fuels due to the high oxidative reactivity of the secondary char (Gao et al., 2019). Other uses for HCs include as a soil amendment (Benavente et al., 2022) and adsorbent for water treatment (Goldfarb et al., 2022). HCs have lower pH and surface area compared to pyrolytically produced biochars. These characteristics, in combination with the amorphous and potentially phytotoxic SC, raise questions about the true applicability of HCs to improve soils and remediate water (Masoumi et al., 2021). Conversely, biochar's benefits when used as soil amendments and adsorbents for heavy metals are well documented (Lehmann et al., 2011; Lin et al., 2021).

During pyrolysis, biomass is heated above  $\sim 500~^\circ\text{C}$  in an inert atmosphere to produce a solid biochar, syngas, and bio-oil. Dry feedstocks are advantageous as no pre-drying step is needed. The energetically dense product of pyrolysis is a liquid fuel. However pyrolysis bio-oil is acidic, viscous, unstable, and has low energy density (Chen et al., 2014). While catalytic upgrading yields fuels suitable for blending with petroleum in current infrastructure, most catalysts are costly as they often comprise metal (some precious) oxides (Locatel et al., 2021). Prior work

in the literature demonstrates that – similar to HTC upgrading – clay minerals can serve as inexpensive yet effective catalysts for both *in situ* and downstream upgrading (Ellison and Boldor, 2021; Karod et al., 2022a, 2022b; Wu et al., 2020).

The majority of current literature probes the impact of single thermochemical conversions on a given biomass. Some studies integrate thermochemical conversions with biological and other Waste-to-Energy components (e.g.,geothermal, solar, biological) to maximize energy recovery (Lee et al., 2023), Integrating thermochemical processes may overcome some of the environmental and energetic limitations posed by each process for the production of liquid and solid renewable fuels. This study utilized a cascaded HTC-pyrolysis process where the feedstock (apple pomace, AP, an agro-industrial waste) is first hydrothermally carbonized, then the resulting HC is pyrolyzed. A similar cascaded process enhanced biochars (Lin et al., 2021) and another demonstrated improved pyrolysis bio-oils using HTC as a "pretreatment" for wood and straw biomass (Magdziarz et al., 2020).

The present work explores two approaches to catalyst addition to these cascaded processes (Fig. 1). First, clay was added prior to HTC to produce a heterogeneous HC-clay composite. Second, clay was added to hydrothermally carbonized biomass. Both types of mixtures were then pyrolyzed. Clays added before HTC undergo two thermochemical treatments and were initially hypothesized to increase carbonization, bio-oil deoxygenation, and biochar surface area to a greater extent than the HCs pyrolyzed with the same clays.

AP is a representative feedstock for several reasons. First, there is a small literature on the HTC of AP including HC properties (Başakçılardan Kabakcı and Baran, 2019) and biocrude compounds (Suárez et al., 2020) and one cascaded process (that we could locate) on subcritical water hydrolysis followed by HTC (Paini et al., 2021). Furthermore, the literature underscores the need to remove water prior to AP pyrolysis. As AP has a higher moisture content and lower energy content than many agro-industrial biomasses and high pyrolytic activation energy resulting in low value fuels, pyrolysis alone is not an optimal waste management strategy (Awasthi et al., 2021). Because HTC increases hydrophobicity and decreases moisture, it is a potential pyrolysis pretreatment step. This is the first study that looks at both (1) the products of cascaded HTC and pyrolysis of AP and (2) the impact of

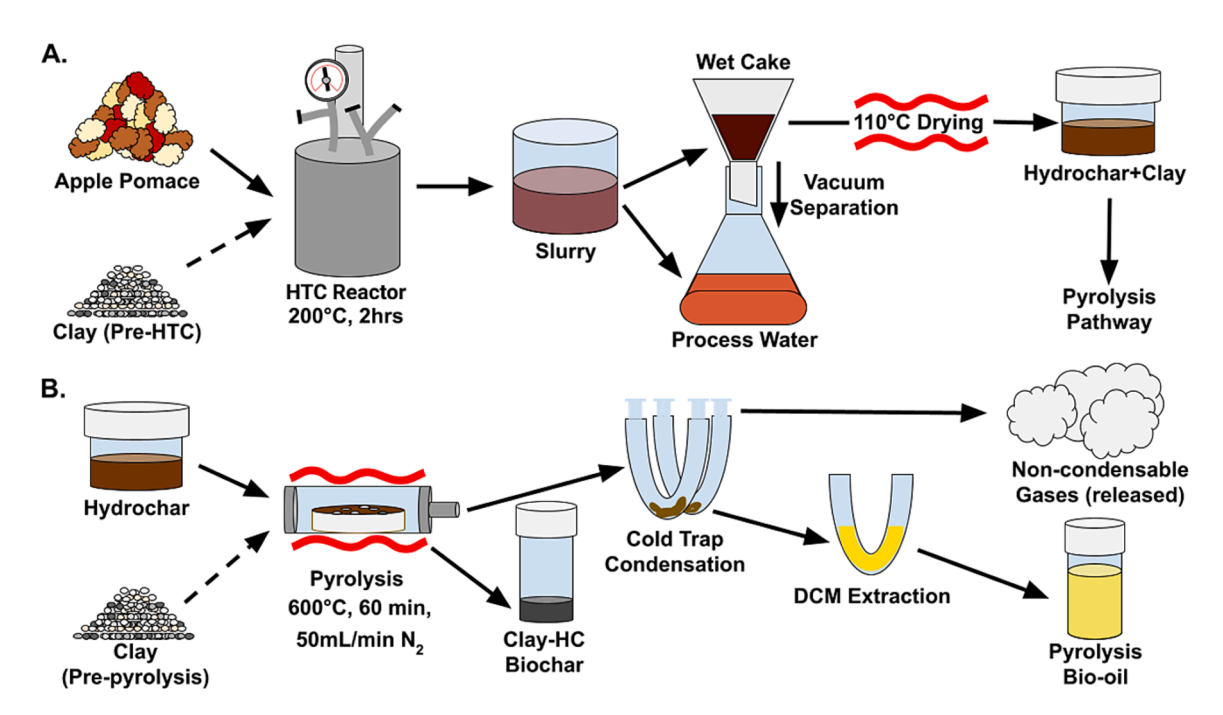


Fig. 1. Exploration of impact of clay addition at two different points in cascaded hydrothermal carbonization and pyrolysis of apple pomace. A. Pathway 1: Addition of clay prior to HTC, followed by pyrolysis of hydrochar-clay composite hydrochars. B. Pathway 2: Addition of clay to hydrochar prior to pyrolysis.

adding two clay minerals, montmorillonite (MMT) and attapulgite (AT), as *in situ* heterogeneous catalysts to upgrade pyrolysis bio-oil when added at different process points.

#### 2. Materials and methods

AP is generated during apple cider, juice, and alcoholic beverage production. It consists of apple flesh, seeds, skins, and some stems (Gowman et al., 2019). Previous analysis shows AP contains  $\sim 11~\%$  hemicellulose,  $\sim \! 14~\%$  cellulose, and  $\sim \! 29~\%$  lignin with some pectin and insoluble fibers (Gowman et al., 2019). Ruby Frost apples (Malus domestica) sourced from the Cornell Orchard were skinned, cored, pulverized, and pressed to create AP, which was stored at  $-4^{\circ}\mathrm{C}$ . Powdered MMT (Alfa Aesar, Montmorillonite K10,  $\mathrm{Al}_2\mathrm{H}_3\mathrm{KO}_{13}\mathrm{Si}_4)$  and AT (Eastchem, 20–40 mesh, Attapulgite,  $\mathrm{Al}_2\mathrm{MgO}_8\mathrm{Si}_2)$  were used as received.

#### 2.1. Hydrothermal carbonization of apple pomace

AP was hydrothermally carbonized, alone and with 10 wt% MMT or AT in a 1 L Parr reactor at 200  $^{\circ}$ C for 2 h. Loading was 500 g with a 15:85 solid (biomass and clay) to water ratio. A reaction temperature of 200  $^{\circ}$ C was chosen as a representative HTC midpoint to demonstrate the cascaded process with clay addition concept. The reactor was cooled by immersing it in a recirculating water bath over approximately 30 min. The resulting slurry was separated via vacuum filtration through filter paper (Whatman 42 mm, 2.5  $\mu$ m) to separate the process water and the solid HC. The HC was dried in a ventilated oven at 110  $^{\circ}$ C for 48 h and the liquid yield was calculated as the process water yield plus the water lost from HC during drying. The gas phase yield was calculated by difference by subtracting the liquid and solid yield from 100 %.

#### 2.2. Pyrolysis of hydrochars

HC samples were pyrolyzed to yield five different biochars: AP biochar with no clay (NC), AP + MMT added pre-HTC (HTC-M), AP + AT added pre-HTC (HTC-A), AP + MMT added between HTC and pyrolysis (PYR-M), AP + AT added between HTC and pyrolysis (PYR-A). PYR-(X) clay addition was 10 % of solid HC mass.

0.5 g samples were placed in a porcelain boat in a 2" horizontal tube furnace (MTI). Nitrogen (Parker Balston, >99.99 %) was flushed through the system at 100 mL/min. The furnace ramped at 10 °C/min until reaching 110 °C, where it held for 30 min to remove residual moisture. The furnace then continued ramping at 10 °C/min to 600 °C, where it held for 60 min. Bio-oil was condensed in a series of cold traps submerged in a dry ice and ethylene glycol mixture. Bio-oil was collected in dichloromethane (DCM). The bio-oil was dried via centrifuging with anhydrous magnesium sulfate and stored at  $-4^{\circ}$ C. Noncondensable gases were analyzed in line after the cold traps with a Quadrupole Mass Spectrometer (Extorr XT Series RGA XT300M) using a fused silica capillary column 45  $\mu$ m in diameter. Solid and liquid mass yields were measured. Each of the five samples were pyrolyzed in triplicate.

#### 2.3. Analysis of pyrolysis products

Bio-oils were analyzed on a Shimadzu GC 2010 Plus Gas Chromatograph-Mass Spectrometer (GC–MS) using a Restek Rtx-5Sil MS 30 m fused silica column. The splitless injection temperature was 230 °C. The oven was held at 40 °C for 5 min, then ramped to 150 °C at 2.5 °C/min, where it was held for 5 min. The temperature then ramped to 250 °C at 0.75 °C/min, where it was held for 10 min, before cooling to 200 °C at -5 °C/min. The MS ion source temperature was 230 °C and the interface temperature was 250 °C. The MS scanned between 15 and 400 m/z after a 6-minute solvent cut time. The resulting peaks were filtered (slopes  $\geq$  500, duration  $\geq$  2 s) and identified by matching spectra ( $\geq$ 70 % match) with the internal NIST libraries. The GC–MS was calibrated

with a series of marker compounds that are common to the pyrolysis of lignocellulosic biomass. Bio-oil from each triplicate pyrolysis run was analyzed on the GC–MS.

Proximate analysis of HCs and biochars was performed using a thermogravimetric analyzer (TGA 5500, TA Instruments). Approximately 6 mg of each sample was placed into a 70  $\mu L$  alumina crucible. Nitrogen flowed through the system at a rate of 25 mL/min. The temperature increased from 25 °C to 110 °C at a rate of 10 °C/min, where it held for 30 min to dry the sample. The temperature then increased to 900 °C at a rate of 10 °C/min, where it held for another 30 min to remove volatile matter. After that, the gas was switched from  $N_2$  to dry air. The temperature ramped again to 950 °C at a rate of 10 °C/min, where it held for 30 min to remove fixed carbon. Residual matter is loosely termed "ash." The instrument was allowed to equilibrate naturally to 40 °C between triplicate runs. Ultimate analysis was performed on a CE-440 Elemental Analyzer (Exeter Analytical Inc.). Sample mass ranged from 1550 to 1850  $\mu g$ . The instrument was calibrated with 3 blanks and 6 acetanilide runs before sample analysis. Samples were run in triplicate.

The pH and electrical conductivity (EC) of the samples were measured in triplicate using the method from Lin et al. (Lin et al., 2021), adapted from the International Biochar Initiative (IBI) (2015). 0.03 g biochar was mixed with 3 mL MilliQ water in 15 mL centrifuge tubes. Tubes were mixed on a shaker table (IKA) at 200 rpm for 2 h. The samples were centrifuged and the supernatant's pH and electrical conductivity (EC) was measured with a SevenExcellence meter (MettlerToledo). The pH probe was calibrated at pH 4 ( $\pm$ 0.01), 7 ( $\pm$ 0.01), and 10 ( $\pm$ 0.01). The EC probe was calibrated at 12.88 µS/cm.

Surface area was measured on a Micromeritics 3Flex adsorption analyzer. Samples were degassed at  $180\,^{\circ}\mathrm{C}$  for  $72\,\mathrm{h}$  under vacuum. Pore volume was measured at a relative pressure of 0.99. BET surface area was measured using five isotherm points between 0.05 and 0.30 relative pressure with confidence intervals reported based on the linear regression of BET curve fitting.

Triplicate FTIR spectra were taken using a Vertex 70 FTIR Spectrometer (Bruker). 200 mg pellets were formed with KBr (Beantown Chemical, FTIR Grade) and the biochar (99:1) in a benchtop press (Carver) under 6 tons of pressure. Samples were analyzed via 64 scans at frequencies ranging from 650 to  $4000 \, \mathrm{cm}^{-1}$ .

#### 2.4. Nutrient bioavailability analysis

Mehlich-III extraction of the chars (Mehlich, 1984) was performed using the same method as Lin et al (Lin et al., 2021). To prevent corrosion and cross-contamination, only polypropylene flasks and plastic pipettes and scoops were used. All reagents were of ACS grade sourced from ThermoFisher. The stock solution was made by adding 6 mL of Millipore ultrapure water (MilliQ water) to a 10 mL volumetric flask. 1.389 g NH<sub>4</sub>F and 0.7306 g ethylenediaminetetraacetic acid (EDTA) were added to the solution, then mixed before bringing the total volume to 10 mL with MilliQ water. In a separate 50 mL volumetric flask, 40 mL MilliQ water was added. Then, 1.000 g NH<sub>4</sub>NO<sub>3</sub>, 0.200 mL stock solution, 0.575 mL of glacial acetic acid, and 0.041 mL of concentrated nitric acid were added, before increasing to 50 mL with MilliQ water. The pH was confirmed to be 2.5 ( $\pm$ 0.1). Triplicate biochar samples were mixed with the solution in a 1:100 (m:v) ratio and shaken at 200 rpm for 15 min. The liquid extractant was removed for analysis.

The biochar Mehlich extracts were digested with nitric acid to remove carbon in preparation for metal analysis using Inductively Coupled Plasma Mass Spectrometry (ICP-MS). Samples were added to Teflon tubes with 20 mL nitric acid (70 %). The tubes were loaded into a microwave digester (CEM) and heated at 195 °C for 30 min. Samples were diluted to a 2 % nitric acid concentration before running on the ICPMS (Shimadzu). Ultra-high purity argon (Airgas) was used as the ICP plasma source and ultra-high purity helium (Airgas) was the carrier gas. The calibration solution used was ICP-MS-68-A-A, which consisted of 48

elements at  $10 \mu g/mL$ , in 2 % nitric acid. The elements studied were B, Na, Mg, Al, P, K, Fe, and Zn, chosen because of their nutritional value.

#### 3. Results and discussion

This work considers two clay catalysts, montmorillonite and attapulgite, as *in situ* catalysts for cascaded HTC and pyrolysis of apple pomace (AP). The impact of the catalysts and when they are added during the thermochemical conversion process (into raw biomass prior to HTC or into HC prior to pyrolysis) is gauged through pyrolysis bio-oil composition and properties of the solid chars produced.

#### 3.1. Thermochemical conversion yields

The HCs with clay incorporated before HTC (HTC-M, HTC-A) had significantly higher biochar yields (p <.05, two tailed t-test) after pyrolysis than the HC-clay mixtures (PYR-M, PYR-A) (Fig. 2). This is because the MMT and AT show minimal devolatilization during HTC while the AP is converted into liquid biocrude, rendering a solid HC with more FC and ash and less VM. Pyrolysis of no clay HC had a solid biochar yield of 32 wt%. From a mass balance perspective, an HC-clay mixture would be expected to have a higher solid yield if it has a higher proportion of clay.

Pyrolysis of raw AP yielded 5.1 wt% bio-oil, which was considerably lower than any other process (p <.05, two tailed *t*-test), and further evidences the unviability of direct wet waste pyrolysis. Direct pyrolysis of raw AP produced a solid yield similar to HTC; however, the remaining mass is largely lost to the gas phase during pyrolysis whereas for HTC the mass is retained in the liquid phase producing a value-added product. While there was relatively consistent total solid conversion among like samples, bio-oil yields varied — the standard deviation of pyrolysis biooil yield ranged from 2.3 % in raw AP to 11.1 % for NC (Table 1). As biogas yields were calculated by difference, this variability propagated, resulting in none of the bio-oil or biogas yields being statistically significantly different between sample types. Residual gas analysis showed high concentrations of H2, CO2, and small hydrocarbons, which have boiling points too low for cold trap condensation. The inability to condense small hydrocarbons may explain the variability in the bio-oil yields as smaller, more fragmented components, are produced. Biochar compositions, as determined via ultimate analysis, showed a decrease in H/C ratio and elemental O percentage from HC to biochar, which corroborates the observed gas production.

#### 3.2. Impact of process and clay insertion on pyrolysis Bio-oil composition

MMT and AT produce similar bio-oils with generally no significant differences between the two clays' oils when they are added at the same process point (Fig. 3). However, bio-oil was affected by the point in which clay was added to the process (before or after HTC). When clay was added to the process pre-HTC (HTC-X), the bio-oil had an average hydrocarbon content of approximately 60 %, whereas adding clay after HTC (PYR-X) showed an average hydrocarbon content of closer to 30 %, similar to the hydrocarbon content in NC bio-oil. Interestingly, this trend appears throughout the bio-oil composition; PYR-M and PYR-A have nearly identical compositions (by functional group) to the NC bio-oil, while the HTC-M and HTC-A samples vary in their average functional group content. There is a notable deviation around the mean for the hydrocarbon groups, the cause for which is not completely clear. We suspect this is due to the overall pyrolysis yields, as discussed above, where smaller hydrocarbons (in particular saturated molecules with 2 and 3 carbons) are not condensed in the cold trap, such that we miss these compounds in bio-oils that have more fragmentation of larger molecules during pyrolysis.

HTC-M showed nearly 0 % ether groups yet HTC-A compounds comprised approximately 20 % ethers. Conversely, HTC-M had approximately 10 % aldehyde groups among its compounds and HTC-A had almost no detectable aldehydes. Despite multiple replicates, these are the only statistically significantly different values within the data, suggesting that these two clays can be used to tune the presence of some functional groups and not others. Future work may explore how different clays' active sites impact functional group presence, but for now we have clearly established that the place of insertion of the catalyst in the cascaded process plays an important role in resulting bio-oil.

A possible explanation for the more varied composition of HTC-X samples is the processing that they have already gone through (HTC). Clay minerals contain active sites in which Lewis or Brønsted acids and bases catalyze reactions such as decarboxylation or deoxygenation through proton or electron donation/acceptance (Oliveira et al., 2021; Reddy et al., 2009). A possible explanation for the low concentration of functional groups in the bio-oil is the deactivation of the catalytic external sites during HTC, which in turn caused low catalytic activity of the clays during pyrolysis. Coking during pyrolysis deactivates aluminosilicate catalysts (Shafaghat et al., 2019), but there are no reports on how coke formation during HTC deactivates catalysts. During HTC, coke (which is essentially secondary char), recondenses onto the surface of the HC to form an amorphous secondary char layer. It is possible that by the point at which HTC-(X) samples are pyrolyzed, the clay catalysts have been largely deactivated due to coke formation, and therefore have

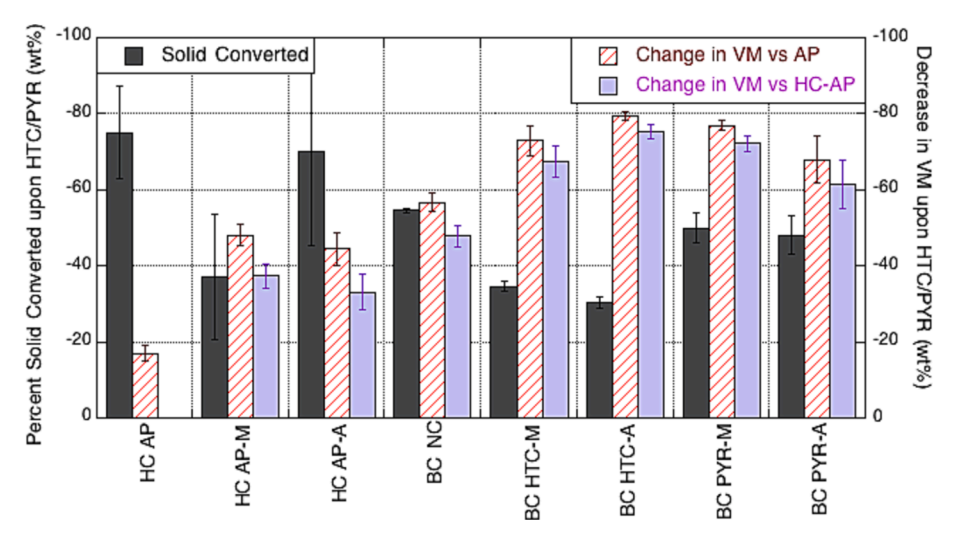


Fig. 2. Total solid and volatile matter conversion and a result of HTC and HTC + PYR (error bars indicate one standard deviation).

Table 1
Yields and characteristics of HTC and pyrolysis of AP-clay mixtures (average of minimum triplicate runs  $\pm$  1 standard deviation) (1 = by difference; 2 = dry basis; 3 = process yield for direct pyrolysis of AP; 4 = dry, ash-free basis).

Char Type	Sample	Process Yield by Phase										Proximate Analysis <sup>2</sup>								
		Solid (wt %)			Liquid (wt %)			Gas <sup>1</sup> (wt %)			VM (wt %)			FC (wt%)			Ash (wt%			
Raw <sup>3</sup>	AP	24.26	±	0.18	5.10	±	2.33	70.58	±	2.48	71.11	±	0.93	23.46	±	0.15	5.43	±	0.88	
Hydrochar	HC AP	25.19	$\pm$	3.80	73.51	$\pm$	3.94	0.83	$\pm$	0.06	59.04	$\pm$	1.75	40.85	$\pm$	1.82	0.10	$\pm$	0.08	
	HC AP-M	64.51	$\pm$	13.47	27.08	$\pm$	6.33	0.82	$\pm$	0.75	36.97	$\pm$	2.62	10.42	$\pm$	2.69	52.62	$\pm$	2.45	
	HC AP-A	29.40	$\pm$	4.15	68.59	$\pm$	5.02	0.56	$\pm$	0.44	39.52	$\pm$	4.31	4.88	$\pm$	3.61	55.60	$\pm$	2.87	
Biochar	BC NC	45.44	±	0.35	31.81	±	11.14	22.75	±	10.79	30.84	$\pm$	2.36	68.70	±	2.52	0.46	$\pm$	0.17	
	BC HTC-M	65.52	$\pm$	0.93	21.45	$\pm$	7.81	13.03	$\pm$	7.12	19.24	$\pm$	3.81	8.52	$\pm$	3.19	72.23	$\pm$	2.53	
	BC HTC-A	69.70	$\pm$	0.71	32.44	$\pm$	4.21	9.25	$\pm$	3.50	14.63	$\pm$	0.57	12.83	$\pm$	0.88	72.54	$\pm$	0.52	
	BC PYR-M	48.72	$\pm$	0.45	26.10	$\pm$	3.19	25.18	$\pm$	2.73	16.44	$\pm$	1.03	67.73	$\pm$	2.38	15.84	$\pm$	3.20	
	BC PYR-A	50.42	±	0.23	24.63	±	5.75	24.95	±	5.74	22.83	$\pm$	6.09	66.51	±	2.18	10.65	$\pm$	7.76	
Char Type	Sample	Ultimat	Ultimate Analysis <sup>4</sup>							IBI Properties										
		C (wt%)			H (wt%)			N (wt%)			O <sup>1</sup> (wt%)			pН			EC (ms/cm)			
Raw	AP	43.22	±	0.44	6.91	±	0.01	0.43	±	0.03	49.44	$\pm$	0.40	5.25	±	0.37	160.21	$\pm$	7.56	
Hydrochar	HC AP	62.27	$\pm$	0.24	4.93	$\pm$	0.02	0.76	$\pm$	0.13	32.05	$\pm$	0.13	4.03	$\pm$	0.04	193.89	$\pm$	2.45	
	HC AP-M	48.91	$\pm$	1.06	5.88	$\pm$	0.21	0.43	$\pm$	0.07	44.80	$\pm$	1.18	5.75	$\pm$	0.15	799.47	$\pm$	0.73	
	HC AP-A	57.57	$\pm$	0.42	6.31	$\pm$	0.95	0.53	$\pm$	0.05	35.61	$\pm$	1.42	5.28	$\pm$	0.06	224.53	$\pm$	5.18	
Biochar	BC NC	85.00	±	1.01	1.84	±	0.09	0.80	±	0.01	12.35	$\pm$	1.11	10.27	±	0.09	126.41	$\pm$	14.26	
	BC HTC-M	79.96	±	4.33	2.56	±	0.07	0.94	±	0.06	16.53	$\pm$	4.39	10.22	±	0.09	112.63	$\pm$	33.57	
	BC HTC-A	74.29	±	8.14	2.51	±	0.10	0.84	±	0.06	22.36	$\pm$	8.30	9.76	±	0.21	48.50	$\pm$	7.36	
	BC PYR-M	72.79	±	0.63	1.68	±	0.13	0.67	±	0.00	24.88	$\pm$	0.69	10.18	$\pm$	0.04	93.21	$\pm$	29.47	
	BC PYR-A	88.61	±	1.82	2.34	±	0.24	0.92	±	0.13	8.14	±	2.10	10.25	±	0.05	121.88	±	30.33	

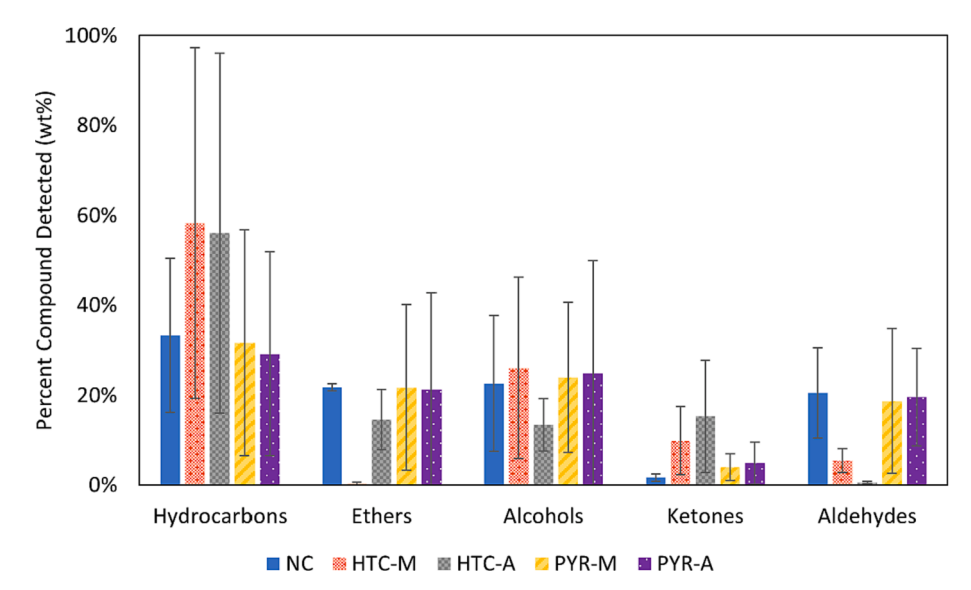


Fig. 3. Composition of pyrolysis bio-oil by functional group as measured by GC–MS (average of triplicate runs  $\pm$  1 standard deviation).

little catalytic impact on bio-oil yield or composition.

Another key takeaway from Fig. 3 is the similarity between NC and PYR-(X) bio-oils. Not only were PYR-M and PYR-A negligibly different from one another, they also were similar to the bio-oil produced from AP HC with no clay (NC). From these observations it appears that clays did not have a (statistically significant) catalytic effect on bio-oil composition. The bio-oils do show potential as a fuel-alternative as they had no carboxylic acids, which has an oxygen to carbon (O/C) ratio of 2. Rather, it was comprised of small, oxygenated compounds which generally have O/C ratios of 1. Biofuels with high oxygen content typically require downstream catalytic deoxygenation. The C=C alkene bonds (614 kJ/mol) have higher energy density than C-H (413 kJ/mol) or C-C bonds (347 kJ/mol), which is favorable in a fuel precursor. Additionally, approximately 30 % of the bio-oil consisted of hydrocarbons (O/C ratio of 0), which could be isolated and used as a sustainable biofuel.

#### 3.3. Hydrochar and biochar characterization

Pyrolysis of HCs yields a biochar with less volatile matter and more

ash than the HC, due to the devolatilization occurring during pyrolysis. Clay catalyst addition increased devolatilization, with each biochar + clay sample showing a greater decrease in VM from AP HC than NC did (p < .05, two-tailed t-test), except for PYR-A (insignificant change). The volatile matter on the HTC-(X) biochars has a higher amount of alcohols, as FTIR analysis (SI) of HTC-(X) biochars had peaks in the 3700-3500 cm<sup>-1</sup> range (O—H stretching) and at 1380 cm<sup>-1</sup> (O—H bending), while the other three (NC, PYR-(X)) had a peak at 1400 cm<sup>-1</sup>. FT-IR spectra of all biochars showed a peak at 1600 cm<sup>-1</sup>, which would indicate C=C stretching, and therefore the presence of alkenes (see supplementary materials). The ash content correlates with the process step the clay is introduced with significant increases from NC, to PYR-(X), then HTC-(X); while this correlates with the fractions of clay that would be in each sample group, there is more ash in the HTC-(X) samples than clay alone could contribute. This result gives evidence hydrothermally carbonizing clays increases their conversion from fixed carbon to ash during the pyrolysis step.

Elemental analysis highlights the carbonizing and deoxygenating effects of the cascaded process. O content was determined via

subtracting the ash content determined via proximate analysis from the residual content in elemental analysis, and was generally lower among clay amended chars, with the exception of PYR-M; O content was under 25 % for all chars (Table 1). The van Krevelen diagram in Fig. 4 shows that both the H/C and O/C ratios decrease after AP undergoes HTC and further after pyrolysis (p <.05, two tailed t-test), whether a catalyst is added or not. O/C ratios were generally lower in samples without clay, likely due to the innate clay O content. While observed O/C was lower for HTC-M than PYR-M, the opposite was true for HTC-A and PYR-A (p <.05, two tailed t-test), implying that deoxygenation is improved when MMT undergoes HTC and AT does not.

HTC-A had a lower pH and electrical conductivity (p < .05, two tailed t-test) than the NC. Except for HTC-A, there were no significant differences in pH or electrical conductivity among the biochars (Table 1). BET surface area measurements (SI) showed that all biochars had significantly higher surface areas than uncatalyzed AP HC (p < .05, two tailed t-test, see supplementary materials). HTC forms an amorphous secondary char which deposits on the primary char (Volpe et al., 2018); this is likely the cause of the reduced surface area. As pyrolysis drives off volatile matter and reopens pore voids, biochar was expected to have a higher surface area than HC as it removes this secondary char (Ischia et al., 2021). HTC-(X) samples had significantly lower surface areas than NC or PYR-(X). The presence of clay in HTC may bind this secondary char to the primary char, creating a structure less prone to pyrolysis; this would explain the increased solid yield among HTC-(X) samples.

#### 3.4. Bioavailability of inorganics and nutrients from chars

ICP-MS was used to measure the bioavailable trace inorganic/metal content in the biochar (Fig. 5). Fig. 5a breaks down this total concentration into its respective elements, while Fig. 5b compares these totals to nutrient bioavailability. Al and B bioavailability increased with the addition of every biochar (p < .05, two tailed t-test). While MMT contains K and AT contains Mg, corresponding increases in total content or bioavailability were not observed. Rather, K bioavailability was significantly higher in PYR-(X) samples than other samples (p < .05, two tailed t-test), and Mg content and bioavailability was significantly higher in HTC-(X) samples than PYR-(X) samples (p < .05, two tailed t-test, see

supplementary materials). This mismatch suggests that the choice of clay catalyst matters less than its treatment, with respect to nutrient bioavailability. Furthermore, it was expected that bioavailability would increase with total inorganic content (and thus a stronger concentration gradient). This pattern roughly held for NC, but in clay amended samples, K and P concentrations were low but their bioavailability was high, as seen in Fig. 5b. As such, the catalysts appear to increase bioavailability.

#### 3.5. Process comparison

Differences in results depended more heavily on clay addition step than clay choice. HTC-(X) samples had higher biochar yields than PYR-(X) or NC, with similar liquid and gas yields. Bio-oil composition was similar between PYR-(X) and NC, while HTC-(X) treatment decreased aldehydes content and increased hydrocarbons (though with relatively high variance among samples). The aqueous phase resulting from HTC contains myriad organic compounds and, industrially, requires significant treatment (Watson et al., 2020). While the aqueous phase was not studied in the present work, further work will examine its treatment for additional energy recovery to improve economic viability. Elemental analysis showed more carbonization and deoxygenation among biochars than HCs, emphasizing the importance of the pyrolysis step in the potential valorization of the solid biochar. HTC-(X) samples had lower BET surface areas than other biochars, possibly due to secondary char incorporation during the HTC step. PYR-(X) samples saw a decrease in total inorganic concentrations, but increased bioavailability.

The present work explored how hydrothermal carbonization and pyrolysis could be coupled in a cascaded pathway to produce bio-oil and biochar. The literature shows clays to have a positive impact on pyrolysis products from other biomass types (Karod et al., 2022b; Ro et al., 2019; Shafaghat et al., 2019). Yet we find that inserting clay prior to HTC, rather than post-HTC (pre-pyrolysis), shows a higher catalytic activity and yields a bio-oil with more desirable hydrocarbons. Future work will explore this for additional biomasses as AP is rather high in sugar and pectin, as compared to other lignocellulosic feedstocks.

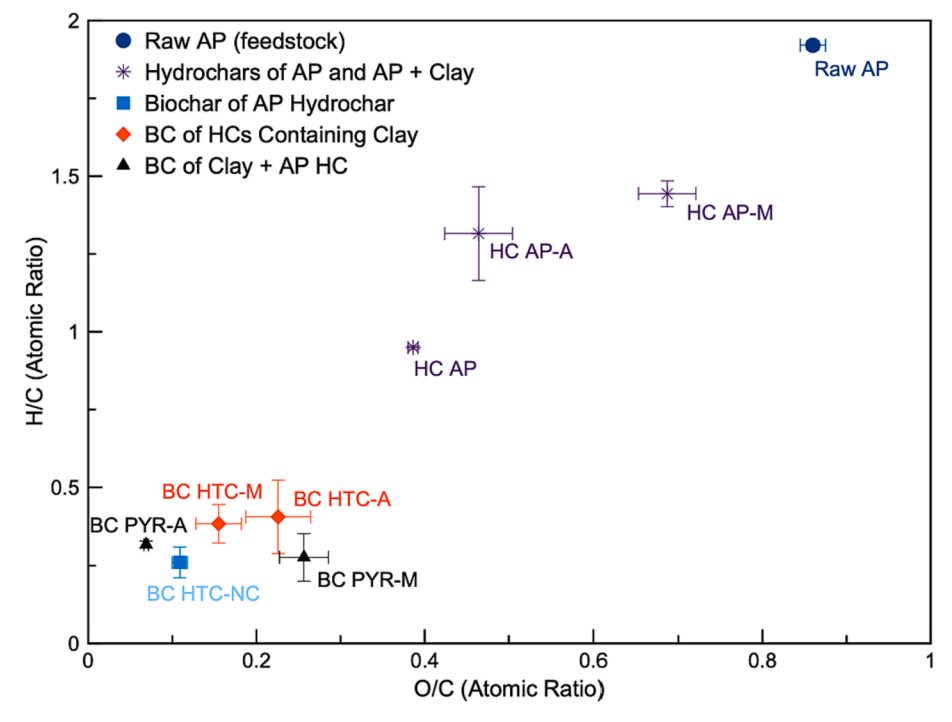
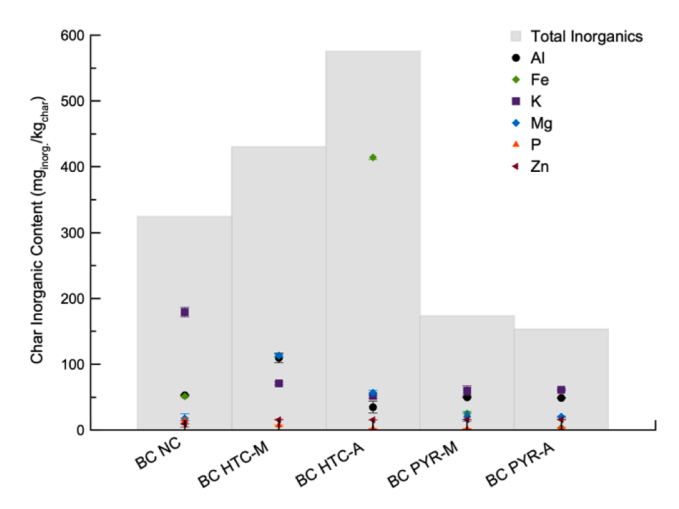
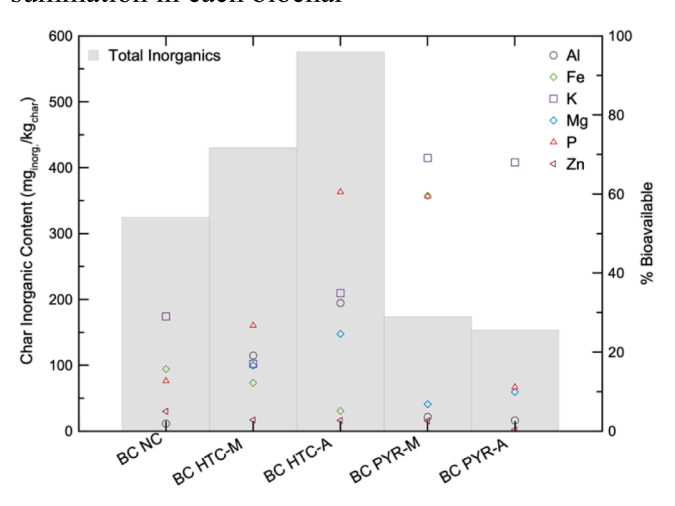


Fig. 4. van Krevelen diagram of raw feedstock and thermochemically processed samples (error bars indicate one standard deviation).



### a. Concentration of six inorganic elements and their summation in each biochar



## b. Total inorganic content (sum of Al, Fe, K, Mg, P, Zn) in each char and percent bioavailability of each element

**Fig. 5.** Concentration of inorganic nutrients and metals in biochars and seedlings and bioavailability as determined via Mehlich-3 extraction (full data, with confidence intervals available in SI).

#### 4. Conclusions

A combined HTC and pyrolysis process was utilized to study the effects of MMT and AT addition, before and after HTC. All catalyst additions showed increased devolatilization in pyrolysis, while clays that underwent HTC decreased carbonization, increased ash and biochar yield. HTC-(X) treatment decreased oxygen content in bio-oil. The HTC-(X) treatment reduced the surface areas of chars though enhanced nutrient concentrations, while PYR-(X) showed decreased nutrient concentrations but higher bioavailability. We found that the addition of clay pre- or post-HTC had little significance on biochar or bio-oil, perhaps due to the homogenous nature of the feedstock or its SC composition.

#### CRediT authorship contribution statement

**James L. Adair:** Methodology, Investigation, Writing – original draft, Visualization. **Madeline Karod:** Methodology, Investigation, Writing – review & editing. **Jillian L. Goldfarb:** Conceptualization,

Methodology, Resources, Writing – review & editing, Supervision, Project administration, Funding acquisition.

#### **Declaration of Competing Interest**

The authors declare that they have no known competing financial interests or personal relationships that could have appeared to influence the work reported in this paper.

#### Data availability

Data will be made available on request.

#### Acknowledgments

This work was supported by a Hatch Grant under accession number 1021398 from the USDA National Institute of Food and Agriculture and by the U.S. National Science Foundation under grant CBET-2031710.

#### Appendix A. Supplementary data

Supplementary data to this article can be found online at  $\frac{https:}{doi.}$  org/10.1016/j.biortech.2023.128649.

#### References

Awasthi, M.K., Ferreira, J.A., Sirohi, R., Sarsaiya, S., Khoshnevisan, B., Baladi, S., Sindhu, R., Binod, P., Pandey, A., Juneja, A., Kumar, D., Zhang, Z., Taherzadeh, M.J., 2021. A critical review on the development stage of biorefinery systems towards the management of apple processing-derived waste. Renew. Sustain. Energy Rev. 143, 110972 https://doi.org/10.1016/J.RSER.2021.110972.

Başakçılardan Kabakcı, S., Baran, S.S., 2019. Hydrothermal carbonization of various lignocellulosics: Fuel characteristics of hydrochars and surface characteristics of activated hydrochars. Waste Manag. 100, 259–268. https://doi.org/10.1016/j. wasman.2019.09.021.

Benavente, V., Lage, S., Gentili, F.G., Jansson, S., 2022. Influence of lipid extraction and processing conditions on hydrothermal conversion of microalgae feedstocks-Effect on hydrochar composition, secondary char formation and phytotoxicity. Chem. Eng. J. 428, 1385–8947. https://doi.org/10.1016/j.cej.2021.129559.

Chen, D., Zhou, J., Zhang, Q., 2014. Effects of torrefaction on the pyrolysis behavior and bio-oil properties of rice husk by using TG-FTIR and Py-GC/MS. Energy and Fuels 28 (0) 5957 5963

Ding, X., Mahadevan Subramanya, S., Waltz, K.E., Wang, Y., Savage, P.E., 2022. Hydrothermal liquefaction of polysaccharide feedstocks with heterogeneous catalysts. Bioresour. Technol. 352, 127100 https://doi.org/10.1016/j. biortech.2022.127100.

de Rezende Locatel, W., Laurenti, D., Schuurman, Y., Guilhaume, N., 2021. Ex-situ catalytic upgrading of pyrolysis vapors using mixed metal oxides. Journal of Analytical and Applied Pyrolysis 158, 105241.

Ellison, C.R., Boldor, D., 2021. Mild upgrading of biomass pyrolysis vapors via ex-situ catalytic pyrolysis over an iron-montmorillonite catalyst. Fuel 291, 120226.

Gao, L., Volpe, M., Lucian, M., Fiori, L., Goldfarb, J.L., 2019. Does hydrothermal carbonization as a biomass pretreatment reduce fuel segregation of coal-biomass blends during oxidation? Energy Convers. Manag. 181, 93–104. https://doi.org/ 10.1016/J.ENCONMAN.2018.12.009.

Goldfarb, J.L., Hubble, A.H., Ma, Q., Volpe, M., Severini, G., Andreottola, G., Fiori, L., 2022. Valorization of cow manure via hydrothermal carbonization for phosphorus recovery and adsorbents for water treatment. J. Environ. Manage. 308, 114561 https://doi.org/10.1016/j.ienyman.2022.114561.

Gowman, A.C., Picard, M.C., Rodriguez-Uribe, A., Misra, M., Khalil, H., Thimmanagari, M., Mohanty, A.K., 2019. Physicochemical analysis of Apple and Grape Pomaces. BioResources. 14 (2), 3210–3230.

IEA, 2022. World Energy Outlook 2022.

Ischia, G., Fiori, L., Gao, L., Goldfarb, J.L., 2021. Valorizing municipal solid waste via integrating hydrothermal carbonization and downstream extraction for biofuel production. J. Clean. Prod. 289, 125781 https://doi.org/10.1016/J. JCLEPRO.2021.125781.

Karod, M., Hubble, A.H., Maag, A.R., Pollard, Z.A., Goldfarb, J.L., 2022a. Clay-catalyzed in situ pyrolysis of cherry pits for upgraded biofuels and heterogeneous adsorbents as recoverable by-products. Biomass Convers. Biorefinery 2022, 1–13. https://doi.org/ 10.1007/S13399-022-02921-3.

Karod, M., Pollard, Z.A., Ahmad, M.T., Dou, G., Gao, L., Goldfarb, J.L., 2022b. Impact of Bentonite Clay on In Situ Pyrolysis vs. Hydrothermal Carbonization of Avocado Pit Biomass. Catalysts 12, 655. https://doi.org/10.3390/catal12060655.

Lee, J., Lin, K.-Y.-A., Jung, S., Kwon, E.E., 2023. Hybrid renewable energy systems involving thermochemical conversion process for waste-to-energy strategy. Chem. Eng. J. 452, 139218 https://doi.org/10.1016/j.cej.2022.139218.

- Lehmann, J., Rillig, M.C., Thies, J., Masiello, C.A., Hockaday, W.C., Crowley, D., 2011.Biochar effects on soil biota A review. Soil Biol. Biochem. 43 (9), 1812–1836.
- Li, L., Diederick, R., Flora, J.R.V., Berge, N.D., 2013. Hydrothermal carbonization of food waste and associated packaging materials for energy source generation. Waste Manag. 33, 2478–2492. https://doi.org/10.1016/j.wasman.2013.05.025.
- Lin, J.C., Mariuzza, D., Volpe, M., Fiori, L., Ceylan, S., Goldfarb, J.L., 2021. Integrated thermochemical conversion process for valorizing mixed agricultural and dairy waste to nutrient-enriched biochars and biofuels. Bioresour. Technol. 328, 124765 https://doi.org/10.1016/J.BIORTECH.2021.124765.
- Magdziarz, A., Wilk, M., Wądrzyk, M., 2020. Pyrolysis of hydrochar derived from biomass – Experimental investigation. Fuel 267, 117246. https://doi.org/10.1016/j. fuel 2020 117246
- Masoumi, S., Borugadda, V.B., Nanda, S., Dalai, A.K., 2021. Hydrochar: A Review on Its Production Technologies and Applications. Catal. 2021, Vol. 11, Page 939 11, 939. 10.3390/CATAL11080939.
- Mehlich, A., 1984. Mehlich 3 Soil Test Extractant: A Modification of Mehlich 2 Extractant. Commun. Soil Sci. Plant Anal. 15, 1409–1416. https://doi.org/10.1080/ 00103628409367568.
- Oliveira, J.L.F., Batista, L.M.B., Alburquerque dos Santos, N., Araújo, A.M.M., Fernandes, V.J., Araujo, A.S., Alves, A.P.M., Gondim, A.D., 2021. Clay-supported zinc oxide as catalyst in pyrolysis and deoxygenation of licuri (Syagrus coronata) oil. Renew. Energy 168, 1377–1387. https://doi.org/10.1016/J.RENENE.2020.12.098.
- Paini, J., Benedetti, V., Menin, L., Baratieri, M., Patuzzi, F., 2021. Subcritical water hydrolysis coupled with hydrothermal carbonization for apple pomace integrated cascade valorization. Bioresour. Technol. 342, 125956.
- Posmanik, R., Cantero, D.A., Malkani, A., Sills, D.L., Tester, J.W., 2017. Biomass conversion to bio-oil using sub-critical water: study of model compounds for food processing waste. J. Supercrit. Fluids 119, 26–35.

- Reddy, C.R., Bhat, Y.S., Nagendrappa, G., Jai Prakash, B.S., 2009. Brønsted and Lewis acidity of modified montmorillonite clay catalysts determined by FT-IR spectroscopy. Catal. Today 141, 157–160. https://doi.org/10.1016/J.CATTOD 2008 04 004.
- Ro, D., Shafaghat, H., Jang, S.H., Lee, H.W., Jung, S.C., Jae, J., Cha, J.S., Park, Y.K., 2019. Production of an upgraded lignin-derived bio-oil using the clay catalysts of bentonite and olivine and the spent FCC in a bench-scale fixed bed pyrolyzer. Environ. Res. 172, 658–664. https://doi.org/10.1016/J.ENVRES.2019.03.014.
- Saqib, N.U., Baroutian, S., Sarmah, A.K., 2018. Physicochemical, structural and combustion characterization of food waste hydrochar obtained by hydrothermal carbonization. Bioresour. Technol. 266, 357–363. https://doi.org/10.1016/j. biortech.2018.06.112.
- Shafaghat, H., Lee, H.W., Tsang, Y.F., Oh, D., Jae, J., Jung, S.C., Ko, C.H., Lam, S.S., Park, Y.K., 2019. In-situ and ex-situ catalytic pyrolysis/co-pyrolysis of empty fruit bunches using mesostructured aluminosilicate catalysts. Chem. Eng. J. 366, 330–338. https://doi.org/10.1016/J.CEJ.2019.02.055.
- Suárez, L., Benavente-Ferraces, I., Plaza, C., de Pascual-Teresa, S., Suárez-Ruiz, I., Centeno, T.A., 2020. Hydrothermal carbonization as a sustainable strategy for integral valorisation of apple waste. Bioresour. Technol. 309, 123395.
- Volpe, M., Goldfarb, J.L., Fiori, L., 2018. Hydrothermal carbonization of Opuntia ficusindica cladodes: Role of process parameters on hydrochar properties. Bioresour. Technol. 247, 310–318. https://doi.org/10.1016/J.BIORTECH.2017.09.072.
- Watson, J., Wang, T., Si, B., Chen, W.-T., Aierzhati, A., Zhang, Y., 2020. Valorization of hydrothermal liquefaction aqueous phase: pathways towards commercial viability. Prog. Energy Combust. Sci. 77, 100819 https://doi.org/10.1016/j. pecs.2019.100819.
- Wu, Z., Wang, F., Xu, J., Zhang, J., Zhao, X., Hu, L., Jiang, Y., 2020. Improved lignin pyrolysis over attapulgite-supported solid acid catalysts. Biomass Convers. Biorefinery. 10.1007/s13399-020-00667-4.